



An investigation of the behavior of quaternized peripherally tetra mercaptopyridine substituted metallophthalocyanines in the presence of quantum dots

Sharon Moeno, Tebello Nyokong*

Department of Chemistry, Rhodes University, P.O. Box 94, Grahamstown 6140, South Africa

ARTICLE INFO

Article history:

Received 10 June 2010

Received in revised form 29 July 2010

Accepted 18 August 2010

Available online 26 August 2010

Keywords:

Quaternization
Metallophthalocyanine
2-Mercaptopyridine
Singlet oxygen
Fluorescence
Quantum yield
Quantum dots

ABSTRACT

The preparation of quaternized peripherally tetra 2-mercaptopyridine substituted phthalocyanines (Pcs) containing Ga³⁺ (**3**) and In³⁺ (**4**) as central metal ions is reported for the first time in this study. In order to determine the potential of these water soluble complexes as photosensitizers for use in photodynamic therapy, photophysical and photochemical studies were carried out on these compounds. In a water:ethanol solvent mixture fluorescence quantum yields (Φ_F) were 0.27 (**3**) and 0.18 (**4**); triplet quantum yields (Φ_T) were 0.75 (**3**) and 0.84 (**4**), respectively. The triplet lifetimes ranged from 20 to 650 μ s, and were larger in DMSO when compared with those in the water:ethanol solvent mixture. The behavior of both complexes in the presence of quantum dots (QDs) was studied and gave evidence of reduction of the complexes by the mercaptopropionic acid stabilizing agent on the surface of the QDs.

© 2010 Elsevier B.V. All rights reserved.

1. Introduction

Metallophthalocyanines (MPcs) are some of the most flexible organic compounds studied to date. Phthalocyanine (Pc) complexes may be exploited in various fields as dyes, sensors, electronic devices, in non-linear optics and as photosensitizers in photodynamic therapy (PDT) [1–6].

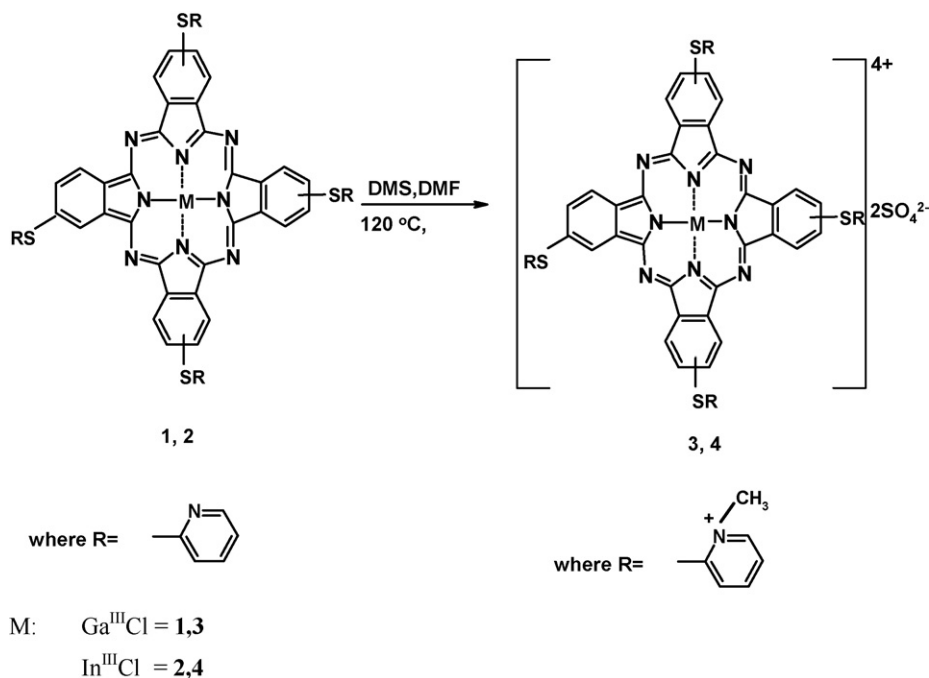
PDT is a treatment for tumours that involves the use of visible light in combination with a photosensitizer and singlet oxygen [6–8]. MPcs are excellent candidates for PDT since they are very photostable, have intense absorption in the red region of the visible spectrum, produce sufficient singlet oxygen, and can be readily cleared from the body once administered [6–9].

MPcs usually have limited solubility in common organic solvents and their solubility is improved by introduction of substituents onto the phthalocyanine ring [10–13]. One way of making MPcs water soluble is by quaternization of the amine functional group on the substituent. The substituents on the Pc ring cause sig-

nificant changes in the photophysical, photochemical and spectral properties of these complexes [10–14]. The nature of the central metal ion also influences to a large degree the photophysical behavior of MPcs. Diamagnetic ions with a closed shell such as Zn²⁺, Al³⁺, Si⁴⁺ result in both high triplet quantum yields (Φ_T) and relatively long triplet lifetimes (τ_T) [15,16].

This work reports on the photophysical properties of the quaternized tetra {2,(3)-(2-mercaptopyridine) phthalocyaninato} (TmTMPyPc, complexes **3** and **4**) complexes of Ga and In, Scheme 1. The MPcs used for quaternization were synthesized and reported on earlier by our group [17]. A study of the behavior of the MPcs in the presence of 3-mercaptopropionic acid stabilized CdTe semiconductor nanoparticles (quantum dots, QDs) [18,19] was carried out to shed light on the actual processes that take place between positively charged MPcs possessing an arylthio substituent and QDs. This investigation was prompted by an earlier study by our group in which two positively charged ZnPcs: one substituted with pyridyloxy and the other with mercaptopyridine substituents, then quaternized, showed different behavior [20] in the presence of QDs. The former showed no changes in the Q band absorption and the latter showed aggregation/reduction in the presence of QDs. The current study will reveal whether the central metal ion, reduction or protonation have any bearing on the peculiar behavior of these positively charged MPcs in the presence of QDs.

* Corresponding author. Tel.: +27 46 6038260; fax: +27 46 6225109.
E-mail address: t.nyokong@ru.ac.za (T. Nyokong).



Scheme 1. Synthetic route of quaternized (2-mercaptopyridine) tetrasubstituted metallophthalocyanine derivatives.

2. Experimental

2.1. Materials

3-Mercaptopropionic acid (MPA) 98%, dimethyl sulfide (DMS), zinc phthalocyanine (ZnPc) and zinc tetra sulfophthalocyanine (ZnTSPc) were obtained from Sigma–Aldrich. Ethanol, N,N-dimethyl formamide (DMF), diethylether, and acetone were obtained from Saarchem. Trifluoroacetic acid (TFA) and dimethyl sulfoxide (DMSO) were obtained from Fluka. The syntheses of (Cl)GaTmTMPyPc (**1**), and (Cl)InTmTMPyPc (**2**) have been reported [17]. 3-Mercaptopropionic acid (MPA) capped CdTe QDs (MPA-CdTe QDs) were synthesized and purified according to reported methods and characterized according to literature [18,21]. The size of MPA-CdTe QDs used in this work is 4.54 nm. Ultra pure water was obtained from a Milli-Q Water System (Millipore Corp., Bedford, MA, USA).

2.2. Equipment

Fluorescence excitation and emission spectra were recorded on a Varian Eclipse spectrofluorimeter. UV–vis spectra were recorded on a Varian 500 UV–Vis/NIR spectrophotometer. IR data were obtained using the Perkin-Elmer spectrum 2000 FTIR spectrometer. ¹H NMR spectra were recorded using a Bruker AMX 400 MHz spectrometer. Elemental analyses were carried out on a Vario EL III MicroCube CHNS Analyzer.

Laser flash photolysis experiments were performed with light pulses produced by a Quanta-Ray Nd:YAG laser providing 400 mJ, 9 ns pulses of laser light at 10 Hz, pumping a Lambda-Physik FL3002 dye (Pyridin 1 dye in methanol). Single pulse energy ranged from 2 to 7 mJ. The analyzing beam source was from a Thermo Oriel xenon arc lamp, and a photomultiplier tube was used as a detector. Signals were recorded with a digital real-time oscilloscope (Tektronix TDS 360). The triplet lifetimes were determined by exponential fitting of the kinetic curves using the program OriginPro 7.5.

Fluorescence lifetimes were measured using a time correlated single photon counting (TCSPC) setup (FluoTime 200, Picoquant

GmbH). The excitation source was a diode laser (LDH-P-C-485 with 10 MHz repetition rate, 88 ps pulse width). Fluorescence was detected under the magic angle with a peltier cooled photomultiplier tube (PMT) (PMA-C 192-N-M, Picoquant) and integrated electronics (PicoHarp 300E, Picoquant GmbH). A monochromator with a spectral width of about 8 nm was used to select the required emission wavelength band. The response function of the system, which was measured with a scattering Ludox solution (DuPont), had a full width at half-maximum (FWHM) of about 300 ps. The ratio of stop to start pulses was kept low (below 0.05) to ensure good statistics. All luminescence decay curves were measured at the maximum of the emission peak. The data were analysed with the program FluoFit (Picoquant). The support plane approach was used to estimate the errors of the decay times [22]. Mass spectra data were collected with a Bruker AutoFLEX III Smartbeam TOF/TOF Mass spectrometer. The instrument was operated in positive ion mode using an *m/z* range of 400–3000. The voltage of the ion sources were set at 19 and 16.7 kV for ion sources 1 and 2, respectively, while the lens was set at 8.50 kV. The voltages for reflectors 1 and 2 were set at 21 and 9.7 kV, respectively. The spectra were acquired using dithranol as the MALDI matrix, using a 354 nm Nd:YAG laser.

2.3. Photophysical studies

2.3.1. Fluorescence quantum yield determinations

Fluorescence quantum yields (Φ_F) were determined by a comparative method [23] using Eq. (1):

$$\Phi_F = \Phi_{F(Std)} \frac{F_{Std} n^2}{F_{Std} A n_{Std}^2} \quad (1)$$

where F and F_{Std} are the areas under the fluorescence curves of the MPc derivatives and the reference, respectively. A and A_{Std} are the absorbances of the sample and reference at the excitation wavelength, and n and n_{Std} are the refractive indices of solvents used for the sample and standard, respectively. ZnPc in DMSO was used as a standard, $\Phi_F = 0.20$ [24], for the determination of fluorescence quantum yields. The sample and the standard were both excited

at the same relevant wavelength. The fluorescence quantum yields for the MPc complexes are represented as $\Phi_{F(\text{MPc})}$ (where MPc represents complex **3** or **4**).

2.3.2. Triplet state quantum yields and lifetimes

Triplet quantum yields were determined using a comparative method based on triplet decay, using Eq. (2) [25]:

$$\Phi_T^{\text{Sample}} = \Phi_T^{\text{Std}} \frac{\Delta A_T^{\text{Sample}} \varepsilon_T^{\text{Std}}}{\Delta A_T^{\text{Std}} \varepsilon_T^{\text{Sample}}} \quad (2)$$

where $\Delta A_T^{\text{Sample}}$ and ΔA_T^{Std} are the changes in the triplet state absorbance of the MPc derivatives and the standard, respectively, $\varepsilon_T^{\text{Sample}}$ and $\varepsilon_T^{\text{Std}}$ are the triplet state extinction coefficients for the MPc derivative and standard (ZnPc), respectively. Φ_T^{Std} is the triplet state quantum yield for the standard, ZnPc in DMSO, $\Phi_T^{\text{Std}} = 0.65$ [26] and the standard ZnTSPc in aqueous media, $\Phi_T^{\text{Std}} = 0.56$ [27]. Φ_T values were determined for the MPcs and are represented as $\Phi_{T(\text{MPc})}$ and the corresponding triplet lifetime as $\tau_{T(\text{MPc})}$.

Quantum yields of internal conversion (Φ_{IC}) were obtained from Eq. (3). This equation assumes that only three processes (fluorescence, intersystem crossing and internal conversion), jointly deactivate the excited singlet state of the ZnPc derivatives.

$$\Phi_{IC} = 1 - (\Phi_F + \Phi_T) \quad (3)$$

2.4. Synthesis

The syntheses of [2,(3)-tetra-(2-mercaptopyridine)phthalocyaninato gallium(III)]Cl (**1**) and [2,(3)-tetra-(2-mercaptopyridine)phthalocyaninato indium(III)]Cl (**2**) have been reported before [17]. This work reports on the quaternization of these MPc complexes using the method by Smith et al. [28].

2.4.1. Quaternized

[2,(3)-tetra-(2-mercaptopyridine)phthalocyaninato gallium(III)]Cl (**3**, (Cl)GaTmTMPyPc Scheme 1)

Compound **1** (0.12 g, 0.11 mmol) was added to DMF (5 mL) and to this solution dimethyl sulfate was added (0.5 mL). The mixture was then left stirring and heated to 120 °C for 12 h under nitrogen. The dark green product was precipitated from DMF with hot acetone, and the precipitate was then washed further with hot acetone, hexane, ethanol and diethyl ether. Yield: 0.041 g (33%). UV/vis (DMSO): λ_{max} nm (log ε): 361 (4.79), 620 (4.56), 691 (5.31); IR (KBr): $\nu_{\text{max}}/\text{cm}^{-1}$: 2997, 2913 ($\nu_{\text{C-H}}$), 1663, 1436, 1406 ($\nu_{\text{C=C}}$), 1311 ($\nu_{\text{C-S-C}}$). ^1H NMR (600 MHz, DMSO- d_6) δ ppm: 9.29–9.26 (4H, m, Pyridyl-H), 8.74–8.68 (8H, t, Pyridyl-H), 8.27–8.21 (4H, d, Pc-H), 7.97–7.93 (4H, d, Pyridyl-H), 7.60–7.45 (dd, 4H, Pc-H), 7.26 (4H, s, Pc-H), 1.29 (12H, s, CH₃). Calcd for C₅₆H₄₀N₁₂S₄GaCl₂SO₄·H₂O: C, 45.55; H, 4.09; N, 11.38; S, 13.04%. Found: C, 44.78; H, 3.95; N, 11.05; S, 17.83%. MALDI-TOF-MS m/z : Calcd: 1078.96; Found: 1078.90 [M]⁺.

2.4.2. Quaternized

[2,(3)-tetra-(2-mercaptopyridine)phthalocyaninato indium(III)]Cl (**4**, (Cl)InTmTMPyPc Scheme 1)

The method employed for synthesis of **4** was the same as the one used for **3**, except compound **2** instead of **1** was employed. The amounts of all the reagents were the same as those used for **3** except the amount of compound **3** (0.095 g, 0.086 mmol). Yield: 0.033 g (38%). UV–vis (DMSO): λ_{max} nm (log ε): 366 (4.75), 626 (4.46), 698 (5.19); IR (KBr): $\nu_{\text{max}}/\text{cm}^{-1}$: 2998, 2914 ($\nu_{\text{C-H}}$), 1709, 1662, 1436, 1407 ($\nu_{\text{C=C}}$), 1311 ($\nu_{\text{C-S-C}}$). ^1H NMR (600 MHz, DMSO- d_6) δ ppm: 9.15–9.13 (4H, m, Pyridyl-H), 9.04–9.03 (4H, d, Pyridyl-H),

Table 1

Absorbance and fluorescence data for MPc complexes in DMSO and aqueous solution (1:1) water:ethanol).

Solvent	MPc	Q band λ_{max} (nm)	Fluorescence emission λ_{max} (nm)	Stokes shift $\Delta\lambda_{\text{Stokes}}$ (nm)	log ε
DMSO	3	691	697	6	5.31
	4	698	702	4	5.19
Water:EtOH	3	686	692	6	5.36
	4	694	698	4	5.16

8.25–8.22 (4H, t, Pyridyl-H), 8.18 (4H, s, Pc-H), 8.05–8.04 (d, 4H, Pc-H), 7.46–7.44 (4H, d, Pc-H), 7.42–7.39 (4H, t, Pyridyl-H), 1.22 (12H, s, CH₃). Calcd for C₅₆H₄₀N₁₂S₄InCl₂SO₄·H₂O: C, 43.91; H, 3.95; N, 10.97%. Found: C, 45.36; H, 3.81; N, 11.21%. MALDI-TOF-MS m/z : Calcd: 1124.06; Found: 1124.60 [M]⁺.

Protonation of the complexes was achieved using trifluoroacetic acid (TFA).

3. Results and discussion

Quaternization of the complexes **1** and **2** to form **3** and **4** was achieved by using a quaternizing agent, dimethyl sulfate (DMS) in DMF at 120 °C to afford methylated derivatives (**3** and **4**). Both complexes exhibited excellent solubility in organic solvents such as DMF and DMSO as well as in aqueous solution. The new compounds were characterized by UV–vis, IR and NMR spectroscopies, MALDI-TOF mass spectra and elemental analysis. The MALDI-TOF mass spectra and elemental analyses are consistent with the predicted structures as shown in Section 2. The mass spectra of the phthalocyanines were obtained by the relatively soft ionization MALDI-TOF technique with the molecular ion peaks observed at m/z 1078.90 for **3** and 1124.60 for **4** with chlorine as the axial atom for both complexes.

The synthesis of the tetrasubstituted MPcs results in the formation of four different isomers which are obtained in an expected statistical mixture, however, no attempt was made to separate the isomeric mixtures of the complexes (**3** and **4**). The ^1H NMR spectra of quaternized tetrasubstituted phthalocyanine derivatives (**3** and **4**) show complex patterns due to the mixed isomer character of these compounds. The complexes were found to be pure by ^1H NMR with all the substituents and ring protons observed in their respective regions.

3.1. Absorption and fluorescence spectral characterization

The UV–vis spectra of the complexes **3** and **4** showed extensive aggregation of these complexes in aqueous media (Fig. 1) as judged by the broad band at 643 nm (for **3**) and 651 nm (for **4**) due to the aggregates, with the monomer peak being observed at 686 nm for **3** (as a shoulder) and at 694 nm for **4**. On addition of ethanol or Triton X-100, complex **3** becomes completely monomeric, this is evidenced by the sharp increase in the intensity of the monomer peak accompanied by a decrease in the intensity of the dimer peak as shown in Fig. 1a. Complex **4** showed monomeric behavior on addition of ethanol, but still showed aggregation in Triton X-100. In DMSO, both complexes were monomeric and obeyed Beer's law for concentrations ranging from 2.0×10^{-6} to 1×10^{-5} M. There is a red shift in the Q band with increase in size of the central metal, thus the Q band position of the monomeric complex **4** (698 nm) is more red shifted than that of complex **3** (691 nm) in DMSO, Table 1.

For both complexes in both DMSO and aqueous solutions, Fig. 2, the excitation spectra are broadened compared to absorption spectra, but are mirror images of the fluorescence emission spectra. The spectral data are shown in Table 1 with Stokes shifts that are small

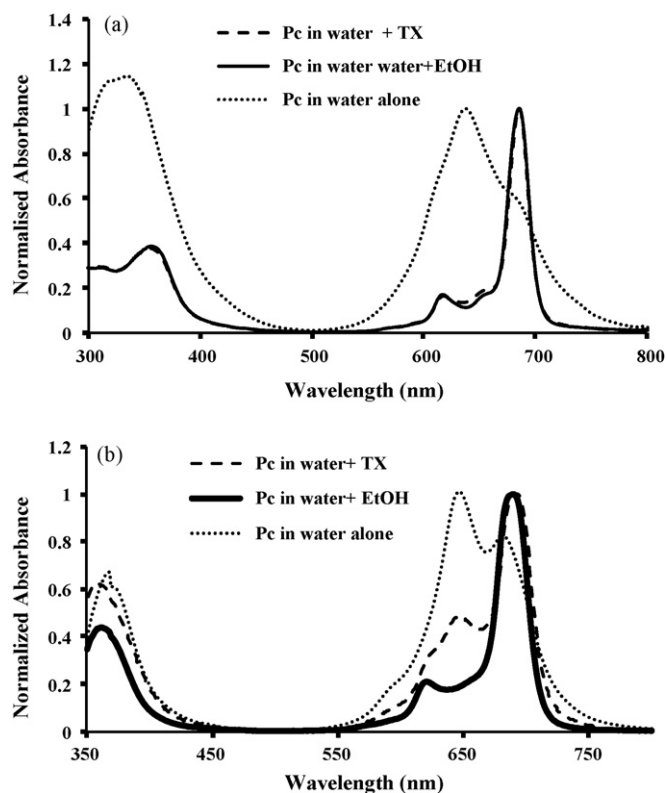


Fig. 1. Absorbance spectra of (a) **3** and (b) **4** in water, (1:1) water:ethanol mixture and in a water and Triton X-100 (TX) solvent mixture.

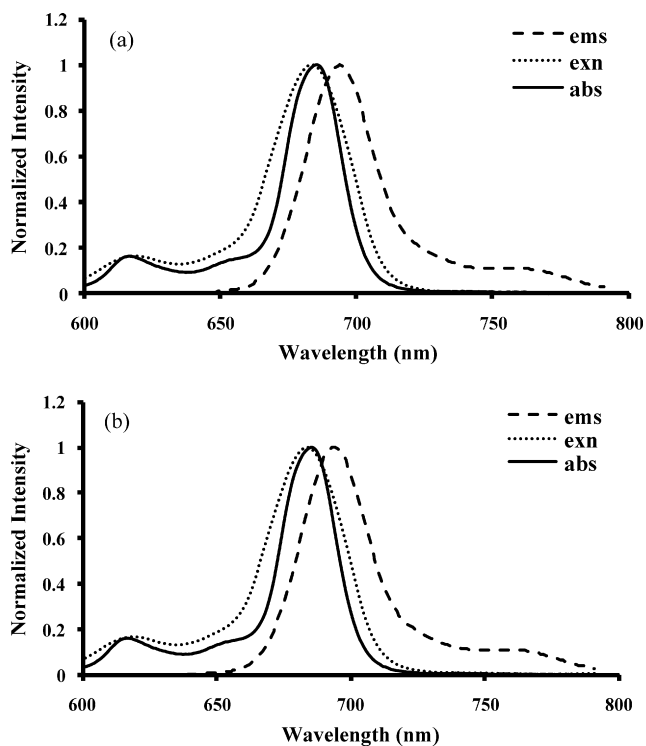


Fig. 2. absorbance (abs), excitation (exn) and emission (ems) spectra of complex **3** in (a) DMSO and (b) (1:1) ethanol:water solvent mixture ($\lambda_{\text{excitation}} = 620$ nm in both solvents used).

Table 2
Photophysical parameters for Tm(Cl)GaTMPyPc (**3**) and Tm(Cl)InTMPyPc (**4**).

Solvent	MPC complex	$\Phi_{F(\text{MPC})}$ $\lambda_{\text{excitation}} = 620$ nm	$\Phi_{T(\text{MPC})}$	$\tau_{T(\text{MPC})}/\mu\text{s}$	Φ_{IC}
DMSO	3	0.25	0.63	650	0.12
	1 ^a	0.30	0.65	110	0.05
	4	0.022	0.68	80	0.42
Water:EtOH	2 ^a	0.030	0.93	60	0.04
	3	0.27	0.75	40	~0
	4	0.018	0.84	20	0.31

^a Data taken from Ref. [17].

and slightly less than values that are typical for MPC complexes in general [14].

Fluorescence quantum yield (Φ_F) values of the MPC complexes are shown in Table 2 for excitation at 620 nm in both DMSO and aqueous solution. The Φ_F values of complex **3** were larger than those for complex **4** in both DMSO and aqueous solution. This is expected since In^{3+} is much larger than Ga^{3+} and hence the former would be expected to encourage intersystem crossing to the triplet state due to the heavy atom effect.

The superimposed absorbance and emission spectra of the 4.54 nm MPA-CdTe QDs used in this work are shown in Fig. 3 and the typical broad absorption and the narrow emission spectra are clearly observed.

3.2. Interaction of complexes **3** and **4** with QDs

The absorption spectral changes resulting from the addition of QDs in small increments to the solution of complexes **3** or **4** in water:ethanol (1:1) solvent mixture or DMSO are shown in Fig. 4a and b, respectively. Similar spectral changes were observed for both complexes in both DMSO and the water:ethanol solvent mixture. The spectral changes observed involved a gradual collapse of the Q band of both complexes **3** and **4** accompanied by the formation of a broad band at 693 nm (for **3**) and 707 nm (for **4**). The red shifting in the spectra could be associated with the rarely observed *J* aggregates which are rare in non-aqueous media [29], and hence are not expected to form in DMSO. The spectral changes observed in Fig. 4, could almost be completely reversed on addition of an oxidizing agent (ferric chloride or bromine). This suggests that the spectral changes are due to reduction in the presence of QDs. The spectral changes, however, do not show the typical spectrum for ring reduced MPC(-2) complexes to form MPC(-3) species, which would consist of the collapse in the Q band and formation of new bands in the 500–650 nm region [30]. In addition, the spectral changes in Fig. 4a and b are quite different from those observed on protonation of aza nitrogens, which occur in acidic media or in the presence of a protonating agent such as TFA [31,32], Fig. 5. Addition

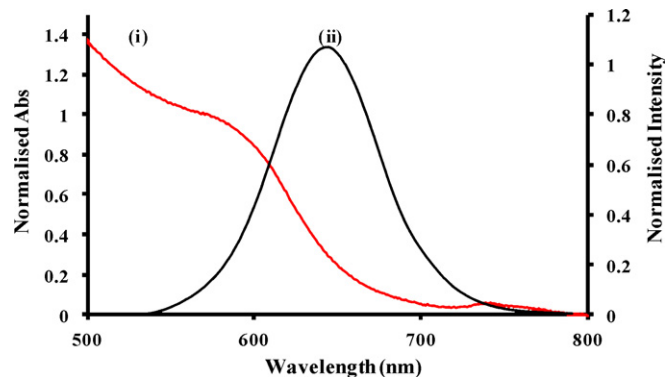


Fig. 3. Absorbance (i) and emission (ii) spectra of CdTe-MPA (1 mg mL⁻¹ in (1:1) ethanol:water solvent mixture, size of 4.54 nm). $\lambda_{\text{excitation}} = 500$ nm.

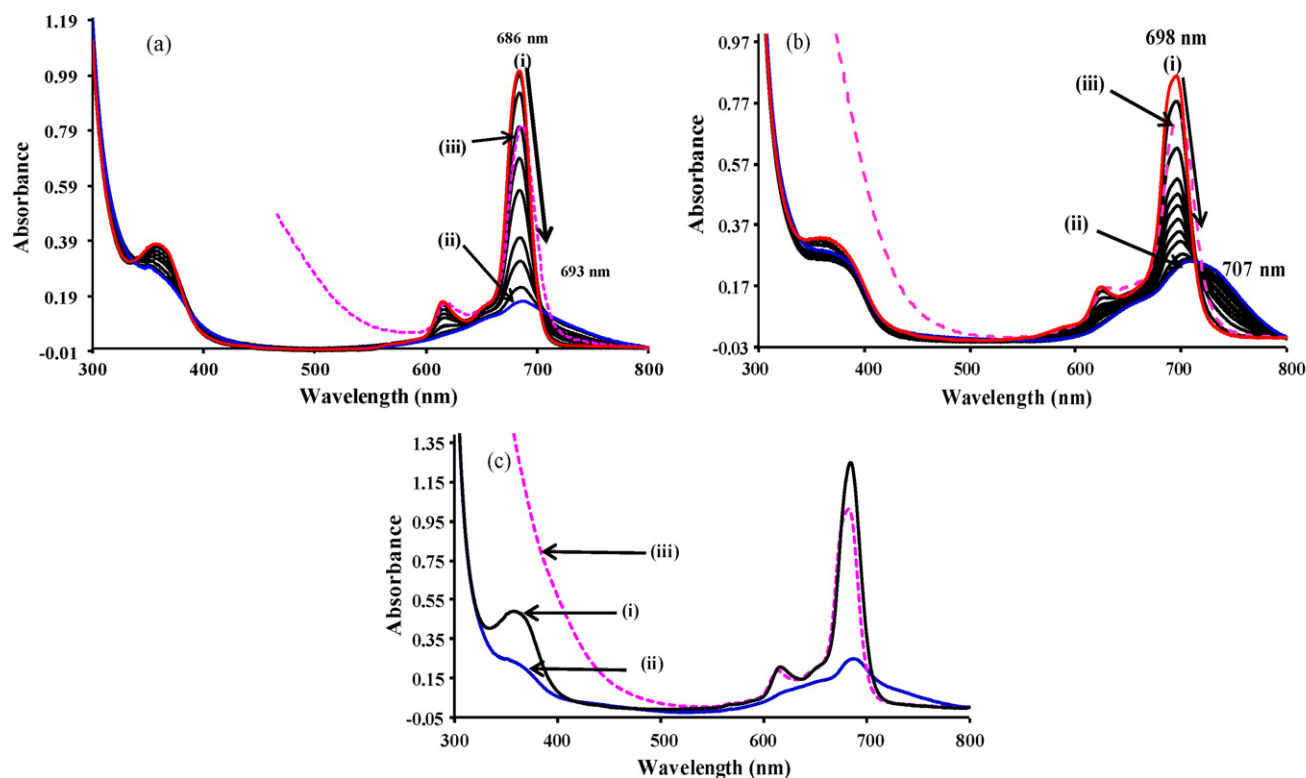


Fig. 4. Absorbance spectral changes upon addition of QDs to (a) **3** in water:ethanol and (b) **4** in DMSO. Spectra before (i) and after (ii) addition of excess QDs (for a and b), and addition of MPA to complex **4** for (c). (iii) Spectra observed on addition of ferric chloride.

of a base (hence deprotonation) to the solution of MPA QDs before adding it to complexes **3** and **4** gave the same spectral changes as shown in Fig. 4a and b. Fig. 4c shows that the addition of the capping agent alone (mercaptopyropionic acid, MPA) resulted in the spectral changes similar to those observed on addition of QDs to solutions of **3** or **4** in that a broad red shifted absorption band was observed at the same position as observed on addition of QDs. The proposed reduction of complexes **3** and **4** by MPA is possible because MPA is also known to be a mild reducing agent [33]. The spectral changes in Fig. 4c could also be mostly reversed by addition of an oxidizing agent as was the case following addition of QDs to complexes **3** or **4**. Thus it is clear that it is not the QDs, but the capping agent which is involved in the transformation of the MPc complexes. Similar behavior was observed for other capping agents such as L-cysteine or thioglycolic acid or their corresponding QDs. The most likely explanation for the spectral changes is that the MPA or MPA QDs reduce the quaternized (hence positively charged) nitrogens on the

pyridine substituents on the ring, since typical spectra due to ring reduction were not observed. For the reported [20] pyridyloxy substituted ZnPc complexes which were also quaternized (positively charged), the spectral changes shown in Fig. 4 were not readily discernible in the presence of MPA QDs but were clearly observed on addition of excess MPA or other capping agents. However, the shifting of the Q band was to the blue (or to red) depending on the type or amount of capping agent. Thus it seems the spectra of positively charged MPc complexes in the presence of QDs depends on many factors such as the linking atom (oxygen versus sulfur) and the central metal. The addition of excess QDs or excess stabilizer MPA significantly quenches the emission spectra of the MPc complexes as can clearly be seen from the example of complex **3** shown in Fig. 6a and b. In Fig. 6, the emission peak for QDs (at 645 nm) is not observed when exciting at 620 nm where both the QDs and the Pc are expected to be excited. The emission peak for QDs is at 645 nm and of the Pc is at 688 nm, there is no peak for the QDs at 645 nm, meaning that the emission of QDs is insignificant on exciting at 620 nm and at the low concentrations of QDs employed. The absorption of QDs at 620 nm is lower than at 500 nm, where the excitation of QDs gave the emission peak at 645 nm.

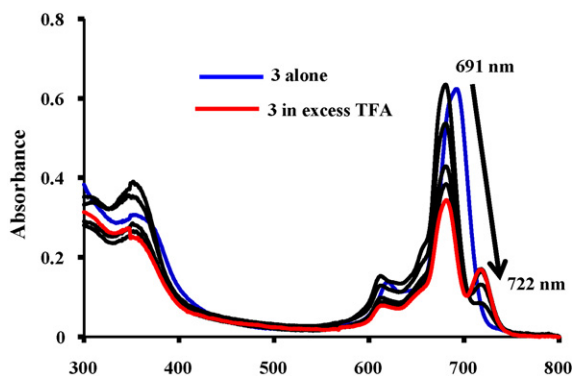


Fig. 5. Absorbance spectral changes upon addition of TFA to complex **3** in DMSO. TFA concentrations increase as follows: 0.71, 1.07, 1.78, 2.14 and 2.85 M.

3.3. Triplet quantum yields (Φ_T) and lifetime (τ_T) studies

The transient absorption spectra were recorded for complexes **3** and **4** in argon degassed DMSO by exciting the MPc photosensitizer in the Q band region and recording the transient absorption spectra point by point from 400 to 830 nm (Fig. 7, using complex **4** as representative). The maximum for triplet state absorption was observed at 520 nm, hence the triplet lifetimes and yields were determined at this wavelength. Fig. 7 (inset) shows a representative triplet decay curve of the complexes. The decay curve obeyed second order kinetics. This is typical of MPc complexes at high concentrations ($>1 \times 10^{-5}$ M) [34] due to triplet–triplet recombination.

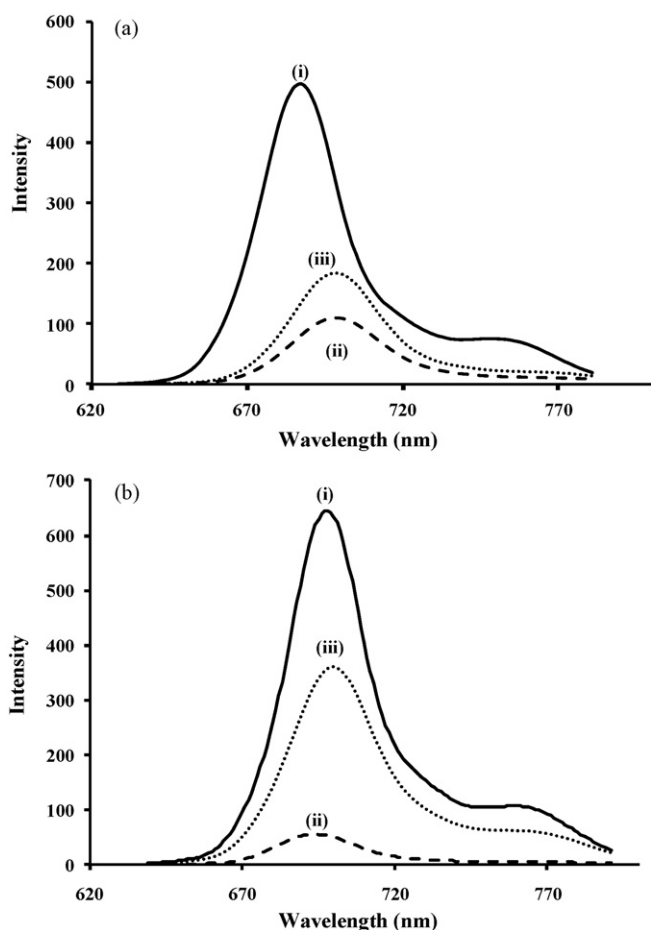


Fig. 6. Emission spectral changes of **3** before (i), after (ii) addition of (a) 3-mercaptopropionic acid (MPA) and (b) MPA QDs. (iii) Addition of bromine to solution of (ii) (solvent (1:1) ethanol:water). [**3**] = 4.5×10^{-6} M, and 5.1×10^{-6} M for (a) and (b), respectively. $\lambda_{\text{excitation}} = 620$ nm.

The concentrations employed in this work were in this range hence triplet–triplet recombination is expected.

The absorption spectra showed evidence of ring reduction with the formation of Pc(-3) species following laser flash photolysis experiments, Fig. 8. Weak absorption bands in the 500–650 nm area in phthalocyanines are typical of ring reduction with the formation of Pc(-3) species [30]. Thus following laser flash photolysis, the complexes showed phototransformation to Pc(-3) species. The

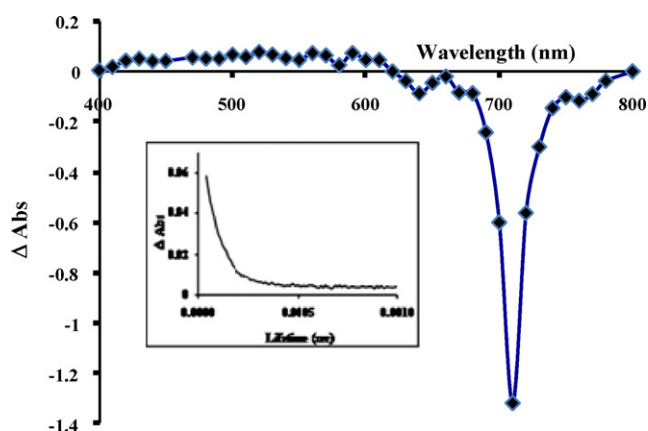


Fig. 7. A transient differential spectrum for **4** in DMSO. Inset: representative triplet decay curve. $\lambda_{\text{excitation}} = 687$ nm in DMSO.

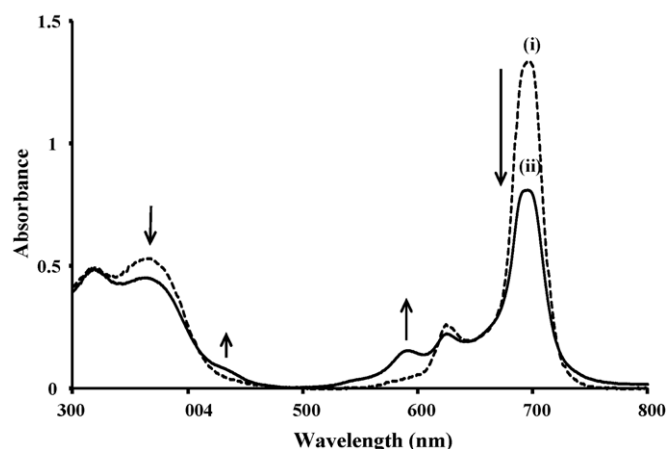


Fig. 8. Absorbance before (i), and absorbance after (ii) laser flash photolysis for **4** in DMSO. $\lambda_{\text{excitation}} = 687$ nm.

observed phototransformation has been reported before by our group [35]. The phototransformation observed for the complexes in DMSO was not observed in the (1:1) ethanol:water mixture. This phototransformation in DMSO affected the triplet quantum yield values in that they are lower than in water:ethanol for complexes **3** and **4**, Table 2.

The Φ_T values were lower for complex **3** compared to complex **4**, in either DMSO or aqueous solution. This trend can be accounted for by the heavy atom effect. Due to the fact that In^{3+} as a central metal ion is heavier than Ga^{3+} it tends to promote movement of a greater proportion of the MPC molecules into the triplet state via intersystem crossing (ISC) resulting in larger Φ_T values than the Ga^{3+} counterpart. A comparison of the current Φ_T values for the quaternized Ga and In complexes with the Φ_T values of the unquaternized molecules previously reported [17] indicates that the unquaternized counterparts have larger Φ_T values than those of the quaternized MPCs in DMSO (values shown in Table 2).

The triplet lifetimes (τ_T) of the MPC complexes were fairly short (Table 2), except for complex **3** in DMSO which showed a large τ_T value (650 μs) which would be expected for smaller central metals such as Al. The lower τ_T value of the MPCs corresponds well with the high value of the Φ_T of the complexes, especially **4**. The trend set by the τ_T values was such that values for complex **3** were considerably higher than those for complex **4** in DMSO and aqueous solution, as expected on the basis of the heavy atom effect. A general observation was that τ_T values were much higher in DMSO compared to aqueous solution. High values of τ_T are preferred as this would give the excited MPC molecules opportunity to stay longer in the triplet state thus allowing for increased collisional interactions between the MPC molecules and ground state molecular oxygen ($^3\text{O}_2$) molecules. This in turn would promote a greater production of singlet oxygen ($^1\text{O}_2$) which is the main cytotoxic species in photosensitized reactions [8]. A comparison of the triplet lifetime values of the quaternized complexes **3** and **4** and the unquaternized complexes shows that the quaternized complexes have much increased lifetimes than their unquaternized counterparts.

3.4. Binding constants and fluorescence quenching

Fig. 9 shows the fluorescence emission spectra of QDs at a known concentration of 0.1 mg/1 mL titrated with varying concentrations of the respective solutions of complexes **3** and **4** (0 – 1.4×10^{-6} M, using Eq. (4) using complex **4** as an example). The QDs were excited at 500 nm (MPC complexes show insignificant emission at this excitation wavelength, since they do not absorb at this wavelength) and fluorescence recorded between 510 and 800 nm. There was a

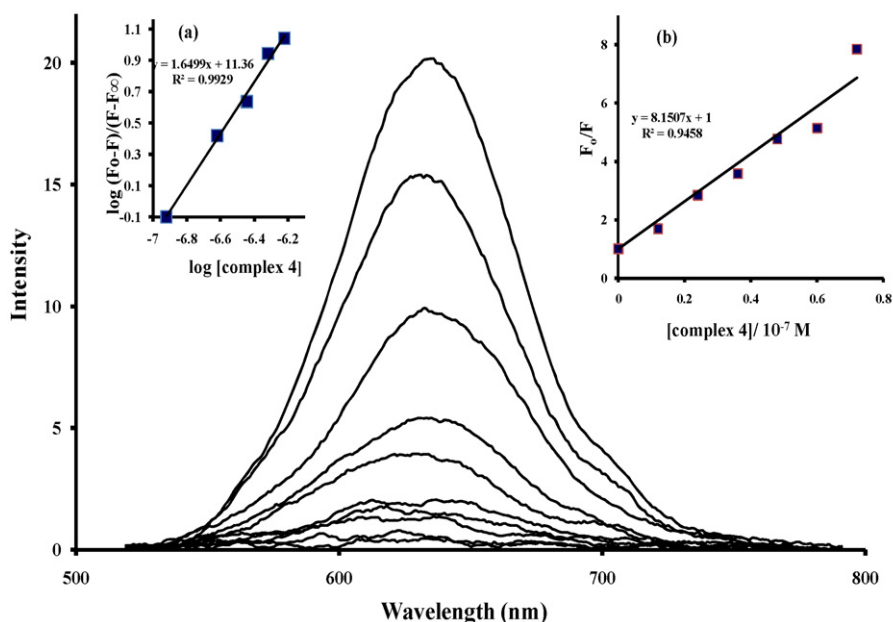


Fig. 9. Variation of the photoemission spectra of CdTe-MPA QDs ($0.1 \text{ mg}/10 \text{ mL}^{-1}$) in the presence of varying concentrations ($0\text{--}9.0 \times 10^{-7} \text{ M}$) of complex **4** in DMSO. Inset (a): plot $\log((F_0 - F)/(F - F_\infty))$ against $\log[\text{complex } 4]$. Inset (b): plot of F_0/F versus $[\text{complex } 4]$. $\lambda_{\text{excitation}} = 500 \text{ nm}$.

steady decrease in the fluorescence intensity of QDs with increase in the concentration of complexes **3** and **4** and this is attributed to fluorescence quenching of the former. The changes in QD fluorescence emission intensities were related to the concentrations of complexes **3** and **4** using the Stern–Volmer relationship shown in Eq. (4) [36]

$$\frac{F_0}{F} = 1 + K[\text{MPC}] \quad (4)$$

where K represents the quenching constant. Fluorescence quenching experiments were carried out and used to determine the binding constants (k_b) and the number of binding sites (n) using Eq. (5) [36–38]:

$$\log \left[\frac{(F_0 - F)}{F - F_\infty} \right] = \log k_b + n \log[\text{MPC}] \quad (5)$$

where F_0 and F represent the fluorescence intensities of QDs in the absence and presence of complexes **3** or **4**, respectively; F_∞ , the fluorescence intensity of QDs saturated with the MPC complexes. Plots of $\log((F_0 - F)/(F - F_\infty))$ against $\log[\text{MPC}]$, Fig. 9 (inset a) provided the values of n (from slope) and k_b (from the intercept). The linearity of the plot shows that the results are in agreement with the Stern–Volmer equation for the range of concentrations that were employed for this study.

The calculated k_b values were in the range of the order of $10^9\text{--}10^{14} \text{ M}^{-1}$, suggesting strong interaction between the MPCs and QDs, Table 3. These values are much higher than reported for the interaction between negatively charged aluminum tetrasulfonated phthalocyanine (AITSPc) with MPA capped QDs of size 3.6 nm, with k_b of $1 \times 10^7 \text{ M}^{-1}$ [39]. QDs are negatively charged and their interaction with positively charged complexes **3** and **4** is expected to be favorable, when compared with their interaction with the negatively charged AITSPc, hence the observed large k_b in the case of complexes **3** and **4**. The k_b values for **4** are larger than for **3** in DMSO. Also the values in aqueous media are larger than in DMSO, this could reflect the ionization status of both the QDs and the MPC complexes in the different solvent media. The static quenching constant values (K) were obtained using Eq. (4) and Fig. 9 (inset b). The values of K were also larger (of the order of 10^7) than reported for the inter-

action of AITSPc with QDs [39] (of the order of 10^5) for the same reasons provided above for k_b .

The value of n was found to be near 2, suggesting that two MPC molecules interact with one QD. The value of $n = 1$ was reported for the interaction of QDs with AITSPc [39], however, smaller QDs were employed for these studies.

3.5. Fluorescence lifetimes

The data from QD fluorescence lifetime measurements are shown in Table 4. A time dependent luminescence intensity decay of the MPA QDs in the aqueous mixture is shown in Fig. 10. The fluorescence lifetime measurements showed the QDs to exhibit a biexponential excitonic emission decay in both solvents used (DMSO and (1:1) water:ethanol solvent mixture). Studies have shown that the shorter lifetimes (fast decay component) are mostly attributed to the excitonic recombination of the core states but the much longer lifetime (slow decay component) usually involve carrier recombination processes in the surface states [40]. As shown in Table 4 the measurements taken in (1:1) water:ethanol solvent mixture show lowering of the longer lifetime (τ_1) of the QDs from 25.4 to 15.3 ns and 6.4 ns upon addition of complexes **3** and **4**, respectively, indicating that the surface states are involved in the quenching process, with complex **4** resulting in greater quenching from 25.4 to 6.4 ns. The observed decrease in lifetimes of QDs in the presence of MPCs for the longer lifetimes (whose recombination is from the surface states), suggests that the quenching process of QDs in the presence of MPC complexes affects the recombination

Table 3

Variation of the binding and quenching constants for the quenching of CdTe-MPA QDs by complexes **3** and **4**.

MPC	Solvent	$k_b/10^{-12} \text{ M}^{-1}$	$K/10^{-7} \text{ M}^{-1}$	n
(3)	DMSO	0.0010	0.82	1.5
	(1:1) H_2O –EtOH	690	2.03	2.0
(4)	DMSO	0.23	8.15	1.7
	(1:1) H_2O –EtOH	286	6.23	2.2

Table 4Fluorescence lifetime measurements from interactions between CdTe-MPA QDs and complexes **3** and **4** in DMSO and aqueous solution ((1:1) water:ethanol).

Sample	Solvent	τ_1^a (ns)	τ_2^a (ns)	α_1^b	α_2^b
MPA QD	H ₂ O–EtOH	25.4 ± 0.2	1.4 ± 0.2	0.86	0.014
MPA QD+ 3	H ₂ O–EtOH	15.3 ± 0.2	1.4 ± 0.05	0.30	0.70
MPA QD+ 4	H ₂ O–EtOH	6.4 ± 0.2	1.4 ± 0.05	0.15	0.85
MPA QD	DMSO	32.0 ± 0.2	4.6 ± 0.3	0.78	0.22
MPA QD+ 3	DMSO	30.6 ± 0.2	3.9 ± 0.2	0.78	0.22
MPA QD+ 4	DMSO	17.7 ± 0.3	3.4 ± 0.1	0.56	0.44

^a Fluorescence lifetimes at MPA QD emission.^b α denotes the amplitude fraction.

from the surface states. It is also worth mentioning at this juncture that the amplitude values (α) give a measure of abundance of species with excitonic recombination within the core of the QD and with recombination from the surface states. Higher amplitudes give an indication of the population of the species at either of the two recombination sites in solution. The results showed that in the aqueous solvent mixture, the species of QD (in the absence of MPc) with recombination processes from the surface states (with τ_1) had a higher amplitude and were thus in greater abundance in solution.

However, upon addition of both complexes **3** and **4**, the species with shorter lifetimes (τ_2) whose recombination is within the core states becomes the more abundant ones in water:ethanol solution. It is important to note that although the abundance of the lifetime within the core states increases, the lifetime itself remains unchanged, it remains at 1.4 ns in water:ethanol solution and this implies that the recombinations within the core states are not involved nor are they affected by the quenching process in the presence of MPc complexes. In DMSO a lowering of the longer lifetime (τ_1) of the QDs from 32.0 to 30.6 ns and 17.7 ns upon addition of complexes **3** and **4**, respectively, is observed. The deduction is that complex **3** does not result in significant quenching of the QD lifetime for the recombination from the surface states but on the other hand complex **4** leads to considerable quenching from 32.0 to 17.7 ns. In DMSO, the species of QDs with recombination processes from the surface states had a high amplitude (α_1) in both the absence and presence of the MPcs and were thus in greater abundance, especially for complex **3**. The shorter lifetimes (τ_2) in DMSO were also slightly lowered in the presence of Pcs as can be seen from Table 4, suggesting that the quenching process occurring at the surface states mildly affects recombination within the core states of the QDs.

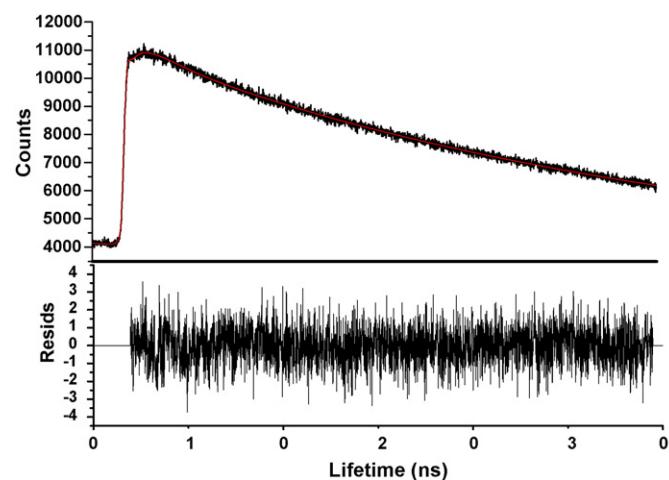


Fig. 10. Photoluminescence decay curve of CdTe QDs in (1:1) water:ethanol solvent mixture ($\lambda_{\text{excitation}} = 645$ nm, measurements taken at the maximum of the exciton emission peak, $\tau_{1/e} = 25.4$ ns).

4. Conclusions

The synthesized CIMTmTMPyPc (M = Ga (**3**) and In (**4**)) complexes are soluble in a some organic solvents, such as DMSO and DMF and they are also soluble in aqueous media. The MPc complexes showed monomeric behavior in DMSO, but were aggregated in aqueous solution. The aggregation was broken by the use organic solvents like ethanol. These complexes had fairly low Φ_F values, but gave high Φ_T values and shorter triplet lifetimes for the complex **4** compared to complex **3** on the basis of the heavy atom effect. The combined photophysical parameters show that these complexes have a potential for use as candidates for applications in PDT.

Acknowledgements

This work was supported by the Department of Science and Technology (DST) and National Research Foundation (NRF), South Africa, through DST/NRF South African Research Chairs Initiative for Professor of Medicinal Chemistry and Nanotechnology as well as Rhodes University. S.M. thanks DAAD foundation for a scholarship.

References

- [1] C.C. Mckeown, Phthalocyanine Materials, Cambridge University Press, 1998.
- [2] E. Ben-Hur, W.S. Chan, in: K.M. Kadish, K.M. Smith, R. Guilard (Eds.), Porphyrin Handbook, Phthalocyanine Properties and Materials, vol. 19, Academic Press, New York, 2003 (Chapter 117).
- [3] D. Dini, M. Barthel, M. Hanack, Eur. J. Org. Chem. 20 (2001) 3759.
- [4] D. Dini, M. Hanack, in: K.M. Kadish, K.M. Smith, R. Guilard (Eds.), Porphyrin Handbook, Phthalocyanine Properties and Materials, vol. 17, Academic Press, New York, 2003 (Chapter 107).
- [5] I. Okura, Photosensitization of Porphyrins and Phthalocyanines, Gordon and Breach Publishers, Germany, 2001.
- [6] R. Bonnet, Chemical Aspects of Photodynamic Therapy, Gordon and Breach Science Publishers, Amsterdam, 2000.
- [7] C.M. Allen, W.M. Sharman, J.E. Van Lier, J. Porphyr. Phthalocyan. 5 (2001) 161.
- [8] J.D. Spikes, J. Photochem. Photobiol. B 6 (1990) 259.
- [9] I.J. Macdonald, T.J. Dougherty, J. Porphyr. Phthalocyan. 5 (2001) 105.
- [10] N. Kobayashi, H. Konami, Phthalocyanines: Properties and Applications, vol. 4, VCH, New York, 1999.
- [11] T. Nyokong, H. Isago, J. Porphyr. Phthalocyan. 8 (2004) 1083.
- [12] A.W. Snow, in: K.M. Kadish, K.M. Smith, R. Guilard (Eds.), Porphyrin Handbook, Phthalocyanine Properties and Materials, vol. 17, Academic Press, 2003 (Chapter 109).
- [13] M. Durmus, T. Nyokong, Photochem. Photobiol. Sci. 6 (2007) 659.
- [14] W. Chidawanyika, A. Ogunsipe, T. Nyokong, New J. Chem. 31 (2007) 377.
- [15] A.C. Tedesco, J.C.G. Rotta, C.N. Lunardi, Curr. Org. Chem. 7 (2003) 187.
- [16] K. Ishii, N. Kobayashi, in: K.M. Kadish, K.M. Smith, R. Guilard (Eds.), The Porphyrin Handbook, vol. 16, Elsevier, 2003 (Chapter 1).
- [17] S. Moeno, T. Nyokong, J. Photochem. Photobiol. A: Chem. 203 (2009) 210.
- [18] N. Gaponik, V.D. Talapin, K. Hoppe, E.V. Shevchenko, A. Kornowski, A. Eychmuller, H. Weller, J. Phys. Chem. B 106 (2002) 7177.
- [19] S. Moeno, M. Idowu, T. Nyokong, Inorg. Chim. Acta 361 (2008) 2950.
- [20] S. Moeno, T. Nyokong, J. Photochem. Photobiol. A: Chem. 201 (2009) 228.
- [21] S. Moeno, E. Antunes, S. Khene, C. Litwinski, T. Nyokong, Dalton Trans. 39 (2010) 3460.
- [22] J.R. Lakowicz, Principles of Fluorescence Spectroscopy, second ed., Kluwer Academic/Plenum Publishers, New York, 1999.
- [23] S. Fery-Forgues, D. Lavabre, J. Chem. Educ. 76 (1999) 1260.
- [24] A. Ogunsipe, J.-Y. Chen, T. Nyokong, New J. Chem. 28 (2004) 822.
- [25] J.H. Brannon, D. Madge, Picosecond laser photophysics. Group 3A phthalocyanines, J. Am. Chem. Soc. 102 (1980) 62.

- [26] P. Kubat, J. Mosinger, *J. Photochem. Photobiol. A* 96 (1996) 93.
- [27] A. Harriman, M.C. Richoux, *J. Chem. Soc. Faraday Trans. II* 76 (1980) 1618.
- [28] T.D. Smith, J. Livorness, H. Taylor, *J. Chem. Soc. Dalton Trans.* (1983) 1391.
- [29] H. Isago, *Chem. Commun.* (2003) 1864.
- [30] M.J. Stillman, in: C.C. Leznoff, A.B.P. Lever (Eds.), *Phthalocyanines: Properties and Applications*, vol. 3, VCH, NY, 1993 (Chapter 5).
- [31] A. Ogunsipe, T. Nyokong, *J. Mol. Struct.* 689 (2004) 89.
- [32] M. Durmus, T. Nyokong, *Spectrochim. Acta A* 69 (2008) 1170.
- [33] B. Karimi, D. Zareyee, *Synthesis* (2003) 1875.
- [34] M.G. Debacker, O. Deleplanque, B. Van Vlierberge, F.X. Sauvage, *Laser Chem.* 8 (1988) 1.
- [35] M. Durmuş, T. Nyokong, *Tetrahedron* 63 (2007) 1385.
- [36] S. Lehrer, G.D. Fashman, *Biochem. Biophys. Res. Commun.* 23 (1966) 133.
- [37] D.M. Chipman, V. Grisaro, N. Sharon, *J. Biol. Chem.* 242 (1967) 4388.
- [38] S.M.T. Nunes, F.S. Sguilla, A.C. Tedesco, *Braz. J. Med. Biol. Res.* 37 (2004) 273.
- [39] M. Idowu, J.-Y. Chen, T. Nyokong, *New J. Chem.* 32 (2008) 290.
- [40] F.S. Wuister, I. Swart, F. van Driel, S.G. Hickey, C.M. Donega, *Nano Lett.* 3 (2003) 503.